



Development of climate tipping damage metric for life-cycle assessment - the influence of increased warming from the tipping

Fabbri, Serena; Owsianiak, Mikołaj; Newbold, Tim; Hauschild, Michael Z.

Published in:
International Journal of Life Cycle Assessment

Link to article, DOI:
[10.1007/s11367-022-02096-z](https://doi.org/10.1007/s11367-022-02096-z)

Publication date:
2022

Document Version
Peer reviewed version

[Link back to DTU Orbit](#)

Citation (APA):
Fabbri, S., Owsianiak, M., Newbold, T., & Hauschild, M. Z. (2022). Development of climate tipping damage metric for life-cycle assessment - the influence of increased warming from the tipping. *International Journal of Life Cycle Assessment*, 27, 1199-1212. <https://doi.org/10.1007/s11367-022-02096-z>

General rights

Copyright and moral rights for the publications made accessible in the public portal are retained by the authors and/or other copyright owners and it is a condition of accessing publications that users recognise and abide by the legal requirements associated with these rights.

- Users may download and print one copy of any publication from the public portal for the purpose of private study or research.
- You may not further distribute the material or use it for any profit-making activity or commercial gain
- You may freely distribute the URL identifying the publication in the public portal

If you believe that this document breaches copyright please contact us providing details, and we will remove access to the work immediately and investigate your claim.

5 **Development of climate tipping damage metric for life cycle assessment –**
6 **the influence of increased warming from the tipping**

7 Serena Fabbri^{1*}, Mikołaj Owsianiak¹, Tim Newbold², Michael Z. Hauschild¹

8

9 ¹Quantitative Sustainability Assessment group, Department of Technology, Management and
10 Economics, Technical University of Denmark, Produktionstorvet, Building 424, DK-2800 Kgs.
11 Lyngby, Denmark.

12 ²Centre for Biodiversity and Environment Research, Department of Genetics, Evolution and
13 Environment, University College London, Gower Street, London WC1E 6BT, UK.

14

15 *Corresponding author.

16 *E-mail address:* serf@dtu.dk (S. Fabbri).

17

18 **Acknowledgments**

19 We thank the European Commission Horizon 2020 project H2020-BBI-JTI-2016: BioBarr, grant
20 agreement 745586 for the financial support during the development of this work.

21

22 **Abstract**

23 **Purpose** The multiple climate tipping points potential (MCTP) is a novel metric in life cycle
24 assessment (LCA). It addresses the contribution of greenhouse gas emissions to disturb those
25 processes in the Earth system, which could pass a tipping point and thereby trigger large, abrupt and
26 potentially irreversible changes. The MCTP, however, does not represent ecosystems damage. Here,
27 we further develop this midpoint metric by linking it to losses of terrestrial species biodiversity at
28 either local or global scales.

29 **Method** A mathematical framework was developed to translate midpoint impacts to temperature
30 increase, first, and then to potential loss of species resulting from the temperature increase, using
31 available data on the potentially disappeared fraction of species due to a unit change in global average
32 temperature.

33 **Results and discussion** The resulting damage MCTP expresses the impacts on ecosystems quality in
34 terms of potential loss of terrestrial species resulting from the contribution of GHG emissions to cross
35 climatic tipping points. The MCTP values range from $2.3 \cdot 10^{-17}$ to $1.1 \cdot 10^{-15}$ PDF (potentially
36 disappeared fraction of species) for the global scale and from $2.7 \cdot 10^{-17}$ to $1.1 \cdot 10^{-15}$ PDF per 1 kg of
37 CO₂ emitted for the local scale. They are time-dependent, and the largest values are found for
38 emissions occurring between 2030-2045, generally declining for emissions occurring toward the end
39 of the century.

40 **Conclusions** The developed metric complements existing damage-level metrics used in LCA and its
41 application is expected to be especially relevant for products where time-differentiation of emissions
42 is possible. To enable direct comparisons between our damage MCTP and the damage caused by
43 other environmental impacts or other climate-related impact categories, further efforts are needed to
44 harmonize MCTP units with those of the compared damage metrics.

45

46 **Keywords**

47 Ecosystems damage modeling, climate tipping points, life cycle impact assessment, global species
48 losses, local species losses, potential disappeared fraction

49

50 **1 Introduction**

51 Life cycle assessment (LCA) aims at quantifying the potential environmental impacts of a product or
52 service over its full life cycle, from extraction of raw materials, through manufacturing and use, to
53 end-of-life (Bjørn et al., 2018). During the life cycle impact assessment (LCIA) phase of an LCA,
54 exchanges between environment and the product system (like emissions of greenhouse gases, GHG)
55 are translated into potential environmental impacts using characterization factors (CF). These

56 exchanges are first summed up and then multiplied by the corresponding substance-specific CF,
57 which represents the impact per unit of emission. CFs are calculated using a model of the underlying
58 impact pathway that connects emissions to environmental damage. These express the potency of an
59 emission in affecting an indicator of the state of the environment that is chosen to represent the
60 environmental impact in question (Hauschild and Huijbregts, 2015). The indicator may be chosen at
61 any point in the impact pathway between emissions and damage to the functioning of ecosystems or
62 human health.

63 In LCA, different types of environmental impacts are analyzed and climate change impacts
64 from emissions of CO₂ and other greenhouse gases released during products' life cycles are often
65 quantified. Emissions of GHGs lead to a change in radiative forcing, i.e. an increase in net energy
66 trapped in the atmosphere, which in turn causes a rise in atmospheric global temperature, which
67 finally causes damage to ecosystems. In this impact pathway, the change in radiative forcing caused
68 by GHGs is typically taken as midpoint (i.e. located in the middle of the impact pathway) indicator of
69 the state of the environment, whereas the final damage to ecosystems (or human health) resulting
70 from the radiative forcing changes represents the endpoint indicator in LCA. The global warming
71 potentials (GWP) proposed by the IPCC are used as midpoint CFs to express the change in radiative
72 forcing induced by GHG emissions over a defined time horizon (typically 100 years) compared to the
73 radiative forcing of carbon dioxide (CO₂) over the same period (expressed in kg CO₂ equivalents). To
74 assess potential damage to ecosystems from GHG emissions, characterization factors modelled at
75 damage (or endpoint) level are used. These are the damage-oriented GWP CFs (calculated as in
76 Huijbregts et al. (2017) starting from the GWP), which allow translating radiative forcing into the
77 resulting time-integrated change in global temperature and finally in damage to either terrestrial or
78 freshwater ecosystems caused by the temperature change.

79 Climate tipping is a relatively new impact category in LCIA (Fabbri et al., 2021; Jørgensen et
80 al., 2014). It offers a complementary perspective to the climate change impact category represented by
81 the GWPs, which consider the time-integrated radiative forcing change but do not link this change to
82 potential crossing of climate tipping points. Indicators of climate tipping, the multiple climate tipping
83 points potentials (MCTP), represent the contribution of a GHG emission to crossing climatic tipping

84 points (observed for processes of the Earth system which may pass a threshold that triggers large
85 abrupt, potentially irreversible changes like change in surface albedo resulting from loss of Arctic
86 Summer sea ice) (Lenton et al., 2008). In the MCTP approach, the contribution to cross tipping points
87 is expressed as contribution of an emission to deplete the remaining carrying capacity of the
88 atmosphere to absorb the GHG impact without crossing a tipping point. As explained in Fabbri et al.
89 (2021), it was modelled by first computing the time-integrated radiative forcing increase from a unit
90 emission of a greenhouse gas; secondly, by converting this radiative forcing increase to atmospheric
91 CO₂-equivalent concentration increase; and finally, by relating the resulting value with the remaining
92 atmospheric capacity, i.e. the remaining increase in atmospheric CO₂-equivalent concentration that
93 can still take place without crossing a tipping point. The result indicates the fraction of remaining
94 capacity occupied by the emission and is expressed as parts per trillion of remaining capacity per unit
95 of GHG emission. The MCTP, however, expresses impacts only at the midpoint level, therefore
96 further developments are necessary to link these midpoint impacts to damage to terrestrial
97 ecosystems.

98 In LCIA, damage modelling for ecosystems traditionally focuses on species biodiversity, and
99 the potentially disappeared fraction of species (PDF) is the most common metric (Curran et al., 2011;
100 Woods et al., 2018). As explained in Verones et al. (2020), exposure duration is also included in the
101 unit of ecosystem damage, so resulting ecosystem damage is expressed as PDF·yr. It can be also
102 expressed as species·yr, when species density and area of exposed ecosystem are known. As argued in
103 Verones et al. (2020), damage scores in LCA should be interpreted as “an increase in global
104 extinction risk over a certain exposure period of time and not so much as an instantaneous global
105 species loss”. Current damage-oriented characterization factors express biodiversity loss at either
106 local, or regional or global scales, and these are frequently mixed in LCIA methods (Verones et al.,
107 2020). A local (or regional) loss of species occurs within a spatially delimited area and can be
108 reverted through repopulation. Global loss means that the species become extinct across the whole
109 planet, and it is thus irreversible. This difference implies that a metric based on local species loss
110 cannot be directly compared with one based on global losses. To avoid comparability issues, it is
111 essential to clearly report at which level new metrics are developed (Jolliet et al., 2018). Local

112 assessments are important to ensure ecosystem functionality while global assessments are necessary
113 to avoid irreversible extinction of species. Thus, the two measures complement each other and it has
114 been argued that characterization factors addressing both scales should be developed for all impact
115 categories (Jolliet et al., 2018; Purvis, 2020; Verones et al., 2020).

116 The aim of this paper is to advance the climate tipping impact category in order to
117 obtain multiple climate tipping points potential (MCTP) at endpoint (damage) level expressing
118 damage to ecosystems, enabling comparison with other damage-oriented impacts. A framework for
119 calculating endpoint MCTP characterization factors is presented for three greenhouse gases (CO₂,
120 methane (CH₄) and nitrous oxide (N₂O)), measuring biodiversity loss at either local or global scale.
121 MCTP factors were computed for three Representative Concentration Pathways, RCP4.5, RCP6 and
122 RCP8.5 representing possible future GHG emission trajectories for the world. The resulting
123 characterization factors, referred to as MCTP_{endpoint}, quantify potential damage to terrestrial
124 ecosystems considering the risk of crossing multiple climatic tipping points. They can be directly
125 applied in LCA studies to assess products and systems and here their application is illustrated with a
126 simplified case study on degradable plastic polymers.

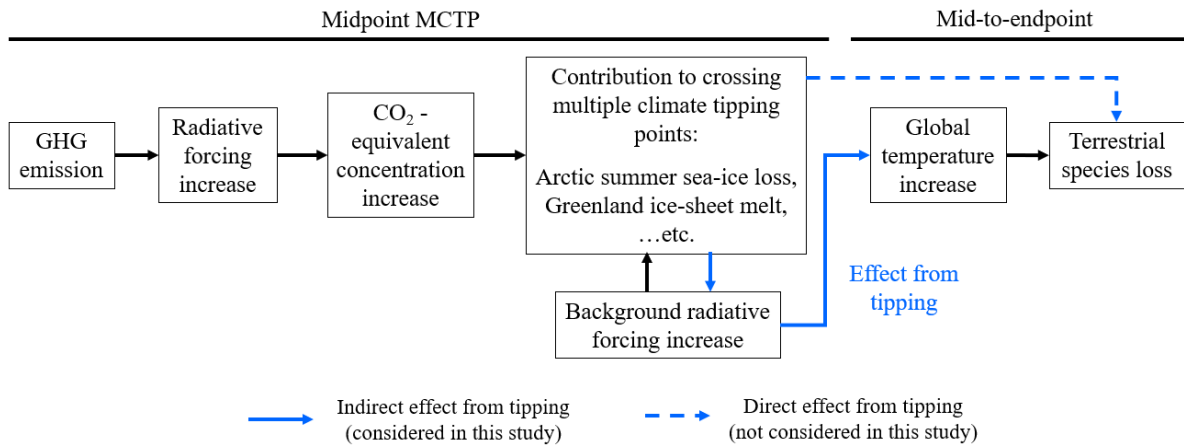
127

128 **2 Methods**

129 **2.1 Impact pathway mechanisms**

130 The midpoint MCTP factor of a unit GHG emission represents the fraction of remaining capacity of
131 the atmosphere to absorb emissions without passing a tipping point that is taken up by the unit
132 emission and is expressed in parts per trillion of remaining capacity per unit emission of a greenhouse
133 gas i (ppt_{rc} · kg _{i} ⁻¹). The midpoint MCTP is then linked to temperature increase per fraction of carrying
134 capacity taken up, and, further on in the impact pathway, to the potential loss of species biodiversity
135 resulting from that temperature increase (see Fig. 1). Note, that in contrast to damage-oriented GWP
136 CFs, which model impacts attributed to marginal GHG emissions (adding on top of the background
137 emissions), damage modeling in the MCTP approach applies an *average* perspective by assuming that
138 an increase in atmospheric CO₂-equivalent concentration is part of the anthropogenic background.

139 Furthermore, the crossing of a given tipping point reduces the remaining carrying capacity for all
 140 subsequent tipping points. This corresponds to an additional temperature increase, which further
 141 contributes to loss of species diversity. Given the current lack of consistent estimates on the direct
 142 effects of crossing tipping points on species loss (through e.g. forest dieback or lengthening of the dry
 143 season), an impact pathway considering only effects from this additional temperature increase is
 144 developed here. The resulting potential loss of species is thus a function of the global temperature
 145 levels resulting from the background emissions and effects from crossing of tipping points on
 146 temperature increase. The $MCTP_{\text{endpoint}}$ CF represents the share that the characterized emission has in
 147 the total predicted species loss.
 148



149
 150 **Fig. 1** Impact pathway for climate tipping used for developing the multiple climate tipping points potential
 151 based on ecosystem damage. Climate tipping has both direct and indirect effects on terrestrial species. Only
 152 indirect effects through global temperature increase are covered in this study.
 153

154 2.2 Modelling framework

155 The endpoint MCTP ($MCTP_{\text{endpoint}}$ in $\text{PDF} \cdot \text{kg}^{-1}$) of a given GHG i emitted at year T_{emission} is derived
 156 from the midpoint MCTP by using a ‘midpoint-to-endpoint’ factor:
 157

$$158 \quad MCTP_{\text{endpoint},i}(T_{\text{emission}}) = MCTP_i(T_{\text{emission}}) \cdot MEF(T_{\text{emission}}) \quad (1)$$

159

160 where $MCTP_i$ [$\text{ppt}_{\text{rc}} \cdot \text{kg}_i^{-1}$] is the multiple climate tipping points potential at midpoint of gas i emitted
 161 at year T_{emission} , and MEF [$\text{PDF} \cdot \text{ppt}_{\text{rc}}^{-1}$] is the midpoint-to-endpoint factor, translating the impact
 162 from contribution to tipping of the emission at T_{emission} to the potentially disappeared fraction of
 163 species [PDF] at either local or global level. Note, that unlike other damage-oriented CFs of climate
 164 impacts (including GWP), exposure duration is not included in the unit of our endpoint MCTP. The
 165 exposure duration is considered when computing time-integrated increase in CO_2 -equivalent
 166 concentration, but it cancels out when the impact is related to the carrying capacity of the atmosphere.
 167 Implications of this on the harmonization of metrics across impact categories will be discussed later
 168 (section 4.2).

169

170 **2.3 Multiple climate tipping potential at midpoint**

171 As in Fabbri et al. (2021), the multiple climate tipping points potential at midpoint, $MCTP_i$ in
 172 [$\text{ppt}_{\text{rc}} \cdot \text{kg}_i^{-1}$] (parts per trillion of remaining capacity taken up by a unit emission) of gas i emitted at
 173 year T_{emission} is defined as the sum of the ratios between the *impact of the emission* and the
 174 corresponding remaining capacity for each of the m tipping points occurring after the emission year:

175

$$176 \quad MCTP_i(T_{\text{emission}}) = \sum_{j=1}^m \frac{I_{\text{emission},i,j}(T_{\text{emission}})}{CAP_j(T_{\text{emission}})} \quad (2)$$

177

178 where j indicates the j th tipping point occurring after the emission year (in order of occurrence) and
 179 can take any value from 1 to m , which is the total number of tipping points that are predicted to be
 180 crossed under the assumed background emission pathway (RCP); $I_{\text{emission},i,j}$ is the *impact of the*
 181 *emission* of gas i with respect to the j th tipping point, CAP_j is the remaining capacity up to the j th
 182 tipping point, and the emission year T_{emission} can be any year from 2021 (or the year when emissions
 183 are expected to start taking place) up to the year of the last tipping point.

184 Details of computing impact and remaining carrying capacity are presented in Fabbri et
 185 al. (2021). Briefly, the $I_{\text{emission},i,j}$ is computed as the radiative forcing of gas i (RF_i) integrated over

186 time between the emission and the tipping (referred to as the absolute climate tipping potential,
 187 ACTP) [$\text{W}\cdot\text{m}^{-2}\cdot\text{yr}\cdot\text{kg}^{-1}$] divided by the radiative efficiency (RE) of 1 ppm of CO_2 [$\text{W}\cdot\text{m}^{-2}\cdot\text{ppm CO}_2^{-1}$].
 188 The CAP_j [$\text{ppm CO}_2\text{e}\cdot\text{yr}$] represents the increase in atmospheric CO_2 -equivalent concentration that
 189 can still take place before reaching the concentration level (in ppm CO_2e) that may trigger tipping j .
 190 This capacity depends on background anthropogenic emissions, and it can be reduced when preceding
 191 tipping points are crossed.

192

193 2.4 Midpoint to endpoint factor

194 The midpoint-to-endpoint factor, $MEF(T_{\text{emission}})$ as it depends on the emission year, is given by:

195

$$196 \quad MEF(T_{\text{emission}}) = \frac{\Delta TEMP(T_{\text{emission}})}{1 \cdot 10^{12}} \cdot \frac{\Delta PDF(T_{\text{emission}})}{\Delta TEMP(T_{\text{emission}})} \quad (3)$$

197

198 where $\frac{\Delta TEMP(T_{\text{emission}})}{1 \cdot 10^{12}}$ [$^{\circ}\text{C}\cdot\text{ppt}_{\text{rc}}^{-1}$] is the global atmospheric temperature change ($\Delta TEMP$) resulting

199 from one part per trillion reduction of the remaining capacity [ppt_{rc}] (i.e., per unit of the midpoint

200 MCTP) and $\frac{\Delta PDF(T_{\text{emission}})}{\Delta TEMP(T_{\text{emission}})}$ [$\text{PDF}\cdot^{\circ}\text{C}^{-1}$] is the rate of potential species loss, at either global or local

201 level ($\text{PDF}_{\text{global}}$ and $\text{PDF}_{\text{local}}$ respectively), per unit change in global average atmospheric temperature.

202 The factor $1 \cdot 10^{12}$ [$\text{ppt}_{\text{rc}}^{-1}$] is needed to re-convert the midpoint $MCTP_i$ into unitless fraction of

203 remaining capacity. Note that both $\Delta TEMP$ and ΔPDF depend on the emission year.

204 The factor $\frac{\Delta TEMP(T_{\text{emission}})}{1 \cdot 10^{12}}$ quantifies the link between the fraction of remaining

205 capacity eaten up by the emission occurring at T_{emission} (calculated by the midpoint MCTP) and the

206 temperature increase associated with taking up that fraction of remaining capacity. To relate these two

207 variables, we consider the overall remaining capacity from the emission year (T_{emission}) up to the

208 year when the last possible tipping point is exceeded (under the assumed background emission

209 pathway) and the average temperature change expected to occur over the same period (eq. 4).

210

$$211 \quad \frac{\Delta TEMP(T_{\text{emission}})}{1 \cdot 10^{12}} = \frac{TEMP(T_{\text{tipping},j_{\text{last}}}) - TEMP(T_{\text{emission}})}{1 \cdot 10^{12}} \quad (4)$$

212

213 where $TEMP(T_{\text{tipping},j_{\text{last}}})$ is the temperature in the year when the last tipping point is exceeded and
 214 $TEMP(T_{\text{emission}})$ is the temperature in the emission year. $\Delta TEMP$ results from the combination of
 215 the background evolution of GHG emissions according to the assumed background emission pathway
 216 and the effect of crossing tipping points. Note, that in eq. 4 the remaining capacity ($1 \cdot 10^{12}$ ppt_{rc}) is
 217 independent of the emission year. It represents the total capacity that is left up to the last tipping point
 218 at each considered emission year.

219 The factor $\frac{\Delta PDF(T_{\text{emission}})}{\Delta TEMP(T_{\text{emission}})}$ represents the rate of potential species loss per unit of
 220 temperature increase. The change in potentially disappeared fraction of species $\Delta PDF(T_{\text{emission}})$ is
 221 calculated as the difference between the foreseen fraction of species lost (F_{lost}) at the highest
 222 considered temperature increase, corresponding to that expected at the last tipping point,
 223 $F_{\text{lost}}(T_{\text{tipping},j_{\text{last}}})$, and the foreseen fraction of species lost at the emission year, $F_{\text{lost}}(T_{\text{emission}})$ (eq.
 224 5).

$$225 \quad \frac{\Delta PDF(T_{\text{emission}})}{\Delta TEMP(T_{\text{emission}})} = \frac{F_{\text{lost}}(T_{\text{tipping},j_{\text{last}}}) - F_{\text{lost}}(T_{\text{emission}})}{TEMP(T_{\text{tipping},j_{\text{last}}}) - TEMP(T_{\text{emission}})} \quad (5)$$

226

227 Studies estimate that this rate is not constant but accelerates as global temperature levels rise (see
 228 section below). This acceleration is accounted for by calculating a different rate for each emission
 229 year, so that emissions occurring at higher levels of warming are attributed a higher potential fraction
 230 of species loss per unit of temperature increase caused by the emission. Note that the change in global
 231 atmospheric temperature over time (resulting from both background evolution of GHG concentrations
 232 and crossing of tipping points) is the only climatic parameter that influences the loss of species caused
 233 by a GHG emission. Other climatic variables, such as precipitation, were not directly considered due
 234 to the lack of a clear correlation between 1) changes in these climatic variables and their contribution
 235 to crossing tipping points and 2) the complementary effects that crossing tipping points has on these
 236 variables.

237 Following the approach developed in Fabbri et al. (2021) for calculation of midpoint
238 MCTP, we consider model uncertainties in the exact location of the temperature thresholds that may
239 trigger the identified potential tipping points. $MCTP_{\text{endpoint}}$ factors are thus computed as a function of
240 the emission year using Monte Carlo simulation (10000 iterations), simulating possible developments
241 with different timing and sequence of the tipping points. The considered tipping points are Arctic
242 summer sea ice loss, Greenland ice sheet melt, West Antarctic ice sheet collapse, Amazon rainforest
243 dieback, Boreal forest dieback, El Niño-Southern Oscillation change in amplitude, Permafrost loss,
244 Arctic winter sea ice loss, Atlantic thermohaline circulation shutoff, North Atlantic subpolar gyre
245 convection collapse, Sahara/Sahel and West African monsoon shift, Alpine glaciers loss, and Coral
246 reefs deterioration (Lenton et al., 2008; Steffen et al., 2018). The uncertainties behind each of the 13
247 tipping points and their implementation into the model are presented in Fabbri et al. (2021) and
248 summarized in Table S1 in Supplementary Information-1. Results are given as the geometric mean of
249 the $MCTP_{\text{endpoint}}$ factors calculated over 10000 iterations.

250

251 **2.5 Determination of temperature change**

252 Future temperature changes are obtained from the global mean temperature projections estimated
253 starting from the Representative Concentration Pathways (RCPs) in Meinshausen et al. (2011). The
254 choice of pathway, in particular the projected rate of GHGs concentration increase, strongly affects
255 the magnitude and the trend of the midpoint MCTPs over emission time, potentially influencing the
256 climate tipping performance of products (Fabbri et al., 2021). To reflect how this choice affects the
257 damage due to GHG emissions, we consider the three pathways RCP4.5, RCP6 and RCP8.5 (numbers
258 referring to the resulting radiative forcing [$W \cdot m^{-2}$] in 2100) (van Vuuren et al., 2011). The lower
259 emission path RCP2.6 is excluded as it is deemed unrealistic (Sanford et al., 2014; van Vliet et al.,
260 2009).

261 In addition, we account for the potential temperature change caused by crossing tipping
262 points, starting from the estimated CO_2 -equivalent concentration increase following tipping that was
263 used for computing the midpoint MCTPs. This is relevant for eight of the thirteen tipping points

264 considered, as for the remaining five tipping points there is either lack of data on the consequences of
265 tipping or lack of evidence that tipping could cause a temperature rise (Fabbri et al., 2021). The
266 resulting global temperature rise is obtained by first adding this increment in CO₂-equivalent
267 concentration to the concentration level projected by the RCP, obtaining a new concentration profile.
268 This new profile is then associated to the corresponding temperature profile derived from the RCP
269 pathway. This implies that while the predicted warming based on the baseline RCP projection is
270 anticipated, the maximum expected temperature increase will never exceed that projected by the RCP.
271 Implications of this modeling choice will be discussed in the method's limitations section (section
272 4.3).

273

274 **2.6 Determination of fraction of species lost**

275 The potentially disappeared fraction of species per unit change in global average temperature,
276 $\frac{\Delta PDF(T_{\text{emission}})}{\Delta TEMP(T_{\text{emission}})}$, is derived from studies that estimate species loss under a given emission pathway
277 (Newbold, 2018; Urban, 2015). Here we consider both measures of local species loss, when species
278 are lost locally but with possible reintroduction from neighboring regions, and global species loss,
279 when species become globally extinct and there is no possibility for recolonization.

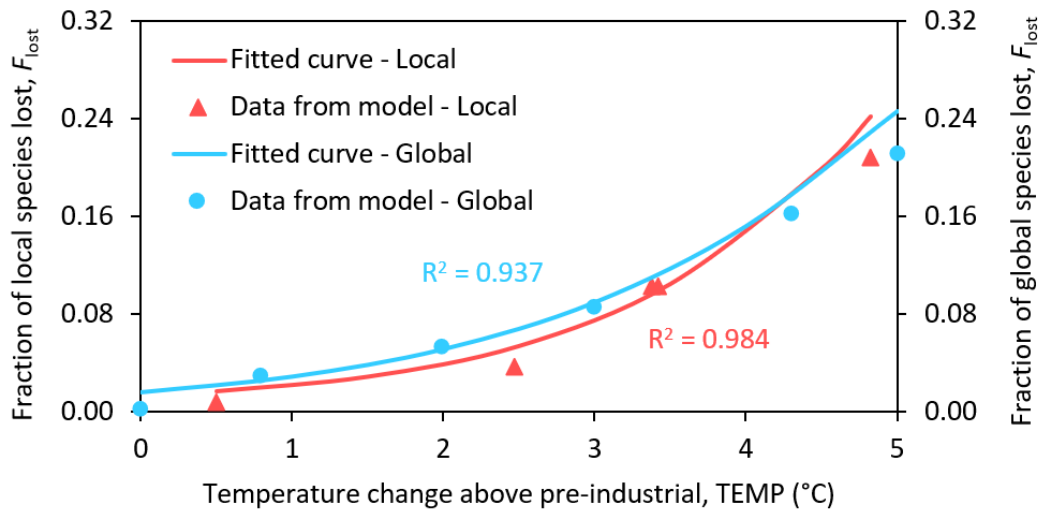
280 Local species loss due to climate change is obtained from Newbold (2018), who
281 calculated global average local losses of terrestrial vertebrate biodiversity for four RCP pathways. It
282 was chosen as one of the most recent studies focusing on climate change effects on local biodiversity
283 loss globally, from which it was possible to obtain sufficient data points to derive a curve relating
284 average local losses of species to changes in global mean temperature. Newbold (2018) developed
285 species distribution models (Elith and Leathwick, 2009) for approximately 20,000 species of
286 amphibians, reptiles, mammals and birds, to estimate local losses (across 10-km² grid cells) in
287 response to climate change. These models relate estimates of species distributions across the entire
288 terrestrial surface of the world to bioclimatic data within each 10-km² grid cell, to predict species'
289 distributions under future climates (Newbold, 2018). Estimated local losses are averaged across all
290 terrestrial areas of the world to obtain a global average. A species is considered lost from a certain

291 area when that area becomes climatically unsuitable for that species, offset by colonization of new
292 species for which that area has become climatically suitable (as long as those species are estimated to
293 be able to reach the area by dispersal). By combining the losses predicted based on the future
294 evolution of four climate variables with the temperature change expected in 2070 under a given RCP,
295 the study shows that temperature increases of 2, 3 and 4.3°C relative to 1960 – 1990 would lead, on
296 average across terrestrial areas and assuming intermediate dispersal ability, to 3, 10 and 20% local
297 loss of species, respectively.

298 Global species loss is taken from a large synthesis of studies predicting extinction risk
299 from climate change carried out in Urban (2015). This study was chosen as it provides the most
300 comprehensive and recent estimates of global species loss from climate change and has already been
301 used to develop damage-oriented GWP factors in the ReCiPe 2016 and LC-IMPACT methods
302 (Huijbregts et al., 2017; Verones et al., 2020, 2019). Urban (2015) compiled 131 predictions covering
303 seven taxonomic groups (plants, invertebrates, amphibians, reptiles, birds, mammals and including a
304 few studies on fish), different dispersal abilities and different modeling techniques to derive the global
305 mean extinction rate per unit of future global temperature rise. Global losses of 3, 5, 8, 16 and 21%
306 are expected for temperature increases of respectively 0.8, 2, 3, 4.3 and 5°C above pre-industrial
307 levels.

308 To integrate the models of Newbold (2018) and Urban (2015) with our midpoint
309 MCTP factors while enabling Monte Carlo simulations, simplified linear regressions were developed
310 based on predictions from the original models of Newbold (2018) and Urban (2015). The regressions
311 predict fraction of species lost (logit-transformed) from temperature change. Details of the regression
312 analyses (i.e., logit-transformation, parameters of the fitted curve, goodness-of-fit statistics) are
313 presented in the Supplementary Information-1 (section S2). Fig. 2 shows predictions of the regression
314 models. Predictions at local and global scale show high similarity in trend and magnitude, implying
315 that the resulting MCTP_{endpoint} factors will not be significantly different from each other in terms of
316 numerical values.

317



318

319 **Fig. 2** Fraction of local and global species lost (F_{lost}) as a function of global temperature change above pre-
 320 industrial levels, $TEMP$. ‘Data from model’ refers to the pairs of values linking a change in species loss with a
 321 change in temperature retrieved from Newbold (2018) and Urban (2015) and found in Table S2 (in
 322 Supplementary Information-1). Since both reference studies for local and global species loss do not provide
 323 estimates beyond 5°C, computations of the $MCTP_{endpoint}$ under RCP8.5, which is the only pathway where
 324 temperature projections exceed 5°C, terminate at the year when the temperature level reaches 5°C in each
 325 iteration

326

327 2.7 Case study

328 Application of the MCTP characterization factors is expected to have particular relevance when
 329 studying the performance of products that have GHG emissions occurring over extended periods of
 330 time, such as slowly degrading plastics (Fabbri et al., 2021). We illustrate the application of the
 331 calculated $MCTP_{endpoint}$ factors in an illustrative case study on the end-of-life stage of four types of
 332 degradable plastic polymers. Details on the considered polymers, scenarios and assumptions are found
 333 in Fabbri et al. (2021), and an overview is provided in Table 1. Comparisons between the four plastics
 334 were made based on emissions of CO_2 and/or CH_4 resulting from either incineration or landfilling of
 335 an amount of plastic material containing 0.5 kg of carbon. Such a functional unit based on
 336 equivalence of the carbon content (and related emissions) between scenarios allows to highlight
 337 differences in emission timing that are relevant for application of the MCTP factors. Under the

338 anaerobic conditions typical of municipal landfills, the polymers degrade at different rates, from fast
 339 (90% degradation within 2 years) to very slow (1% degradation within 100 years), resulting in
 340 different CO₂ and CH₄ emission profiles derived from the carbon contained in the polymer (scenarios
 341 2-5 in Table 1). Degradation may also be delayed by several years in landfills (scenarios 6 and 7). In
 342 contrast, during incineration only CO₂ emissions are released and all at the same time (scenario 1).
 343 These differences in emission timing are expected to influence the performance of the polymers when
 344 measured with the MCTP approach. Using the degradation rate constants of the polymers, yearly
 345 emitted quantities of GHGs are calculated, multiplied by the corresponding year-specific average
 346 MCTP_{endpoint} factor per unit emission and summed over the period from the first GHG emission
 347 release (here assumed to be 2021) up to the last tipping point ($T_{\text{tipping},j_{\text{last}}}$) and over each GHG i . The
 348 result is the total impact score (IS) in terms of potentially disappeared fraction of species (PDF) from
 349 the end-of-life degradation of plastic (eq. 6):

350

$$351 \quad IS = \sum_i \sum_{T_{\text{emission}}=2021}^{T_{\text{tipping},j_{\text{last}}}} m_i(T_{\text{emission}}) \cdot MCTP_{\text{endpoint},i}(T_{\text{emission}}) \quad (6)$$

352

353 where $m_i(T_{\text{emission}})$ is the mass of GHG i emitted at year T_{emission} . Impact scores are calculated with
 354 the MCTP_{endpoint} factors for both local and global species losses, and calculations are done with CFs
 355 representing each of the three RCPs. For comparison, we also compute impact scores using the
 356 complementary and most commonly used GWP-based metric of damage to terrestrial ecosystems
 357 (damage GWP) included in the LCIA method ReCiPe 2016, where metric scores are expressed in
 358 [species·yr].

359

360

361

362

363 **Table 1** Overview of the seven scenarios considered for the case study with functional limit “average treatment
 364 of 0.5 kg carbon contained in the plastic material”. Adapted from Fabbri et al. (2021)

Scenario	Polymer	Degradation rate constant, k (day^{-1})	Note
1. Incineration	Generic fossil-based	Not relevant	All carbon contained in the polymer is released as CO_2 in year 1
Plastic degradation rate			
2. Fast (90% degradation in 2 years)	Polycaprolactone (PCL) – fossil-based	$2.97 \cdot 10^{-3}$ ^(a)	In total, 71% of the carbon is released as CO_2 and 29% as CH_4 , in different years depending on the degradation rate constant ^(d)
3. Medium (90% degradation in 31 years)	Polybutylene succinate (PBS) fossil-based	$2.02 \cdot 10^{-4}$ ^(b)	
4. Slow (90% degradation in 105 years)	Polystyrene (PS) fossil-based	$6.00 \cdot 10^{-5}$ ^(c)	
5. Very slow (1% degradation in 100 years)	Polylactic acid (PLA) – bio-based	$2.77 \cdot 10^{-7}$ ^(d)	
Delayed degradation			
6. After 20 years (fast rate)	Polycaprolactone (PCL) – fossil-based	$2.97 \cdot 10^{-3}$ ^(a)	Degradation in landfill of the fast-degrading plastic (scenario 2) is assumed to be delayed by 20 and 50 years, respectively.
7. After 50 years (fast rate)	Polycaprolactone (PCL) – fossil-based	$2.97 \cdot 10^{-3}$ ^(a)	

365 ^(a) (Ishigaki et al., 2004); ^(b) (Cho et al., 2011); ^(c) (Tansel, 2019); ^(d) (Rossi et al., 2015).

366

367 **3 Results**

368 The complete set of $\text{MCTP}_{\text{endpoint}}$ values for CO_2 , CH_4 and N_2O calculated for each RCP pathway and
 369 expressed as either local or global species loss are presented in Supplementary Information-2 (Tables
 370 S1-S6). Here, only selected results for CO_2 will be illustrated to facilitate their interpretation. Results
 371 for CO_2 are first presented for a sample iteration (i.e. a Monte Carlo simulation representing a
 372 possible scenario in which nine different tipping elements cross their tipping point) under the RCP6
 373 pathway as an example. To illustrate the influence of the adopted approach on the final $\text{MCTP}_{\text{endpoint}}$
 374 values, results are shown separately for all the factors underlying the calculation of $\text{MCTP}_{\text{endpoint}}$.
 375 Next, results from 10000 Monte Carlo iterations accounting for current uncertainties in tipping
 376 occurrence are presented and compared between RCP pathways. Finally, main outcomes from the
 377 case study are presented. The $\text{MCTP}_{\text{endpoint}}$ values for CO_2 , CH_4 and N_2O can be found in
 378 Supplementary Information-2.

379

380 3.1 MTCPs for a sample iteration

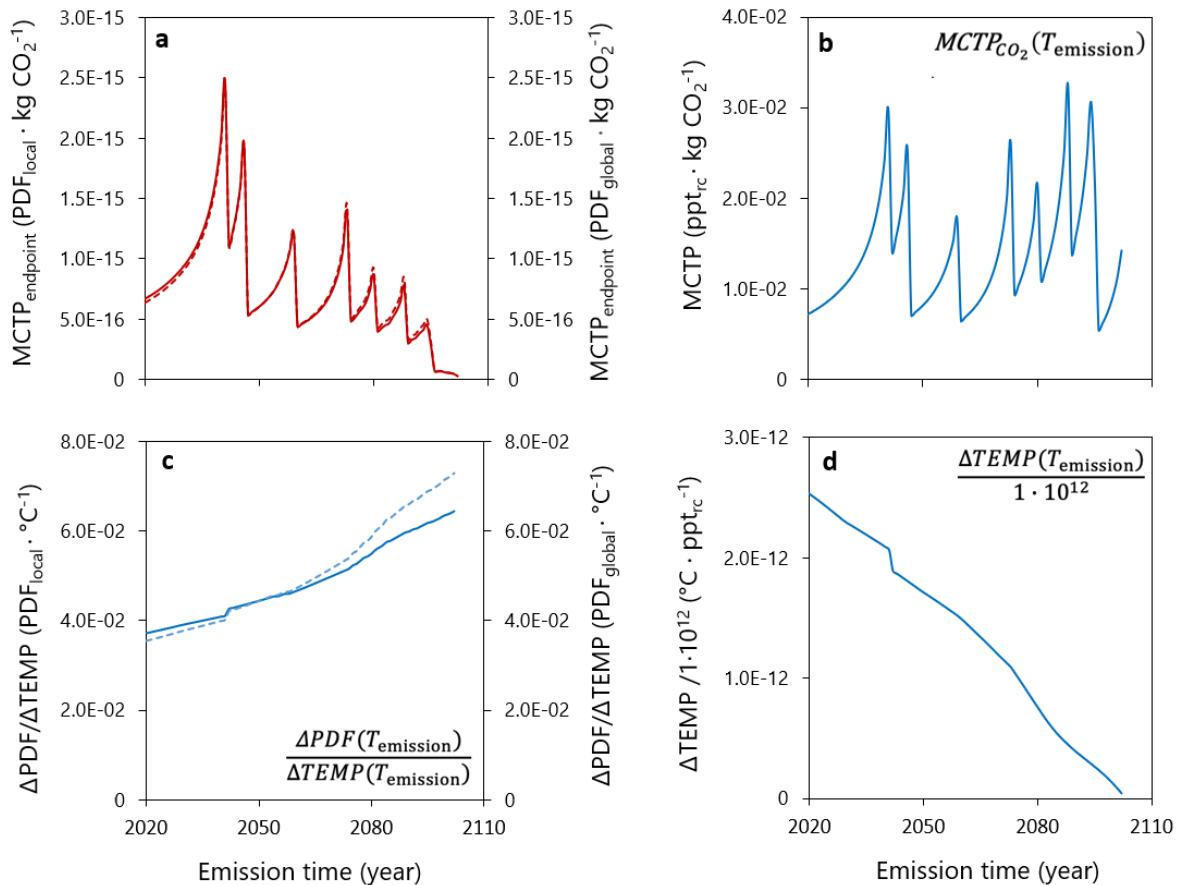
381 Fig. 3a shows $MCTP_{\text{endpoint}}$ factors for CO_2 for a sample iteration in terms of both local and global
382 fraction of species loss, as depending on the time when the CO_2 emission occurs. The first observation
383 is that $MCTP_{\text{endpoint}}$ factors are proportional to their corresponding midpoint MCTP (Fig. 3b) and
384 follow a similar pattern. As already shown in Jørgensen et al. (2014) and Fabbri et al. (2021),
385 midpoint MCTPs peak just before the passing of a tipping point, indicating that the contribution of an
386 emission to cross the tipping point increases as the emission pathway approaches the tipping point.
387 Here, the increase in $MCTP_{\text{endpoint}}$ suggests that an emission occurring before an expected tipping
388 threshold has a higher potential to cause ecosystem damage due to its larger contribution to deplete
389 the remaining capacity and cross the tipping point. On the contrary, emissions after the tipping point
390 have smaller contribution to crossing subsequent tipping points. This is seen as a discontinuity in the
391 $MCTP_{\text{endpoint}}$ curve.

392 $MCTP_{\text{endpoint}}$ values generally increase until ca 2045, but they are almost 2 orders of
393 magnitude lower for emissions occurring toward the end of the century. This decreasing trend is
394 explained by the fact that the temperature change per fraction of remaining capacity taken up by the
395 emission decreases as the emission occurs later in time. Therefore, despite the fact that the potential
396 species loss per unit temperature increase, e.g. in 2070, is expected to be higher than that in 2035 (Fig.
397 3c and Table S3 in Supplementary Information-1), the resulting damage from an emission in 2070 is
398 lower than that in 2035 because the corresponding temperature change induced by that emission is
399 also lower (Fig. 3d). This observation may seem counterintuitive if one would expect larger impact to
400 be computed for emissions occurring later in time (consistently with Fig. 2) but is in line with an
401 *average* approach to modeling of characterization factors for use in LCA. As argued in Fabbri et al.
402 (2021), the MCTP factors represent average impact as they depend on the background level. Thus,
403 averaging temperature change between emission year and year of the last tipping point (making the
404 resulting $\Delta TEMP$ decrease with later emission time) is necessary to calculate indicator scores for
405 emissions occurring at that specific emission year. These emissions cannot be made responsible for

406 the temperature increase and resulting ecosystem damage that happened before the emission year of
 407 interest.

408 Finally, $MCTP_{\text{endpoint}}$ factors calculated using local species loss estimates show little
 409 difference from those obtained using global species loss estimates. Results for local losses are
 410 maximum 13% larger and 5% smaller compared to results for global losses, depending on the
 411 emission time. However, we stress that their interpretation is not the same. Local losses represent
 412 potentially reversible damages through the loss of ecosystem functioning caused by local loss of
 413 species, whereas global extinctions represent irreversible losses of biodiversity (see Section 4.1 for
 414 further discussion).

415



416

417 **Fig. 3** (a) Endpoint MCTP ($MCTP_{\text{endpoint}}$) for emission of 1 kg of CO₂ expressed as Potentially Disappeared
 418 Fraction (PDF) of species at local (dashed line, left axis) and global (solid line, right axis) level in a sample
 419 iteration under RCP6. Note that differences between the two curves are so small that they appear mostly
 420 overlapping. (b) Midpoint MCTP for emission of 1 kg of CO₂. (c) Potentially Disappeared Fraction of species

421 (PDF) at local (dashed line, left axis) and global (solid line, right axis) level per degree Celsius increase in
422 global temperature. **(d)** Temperature change per fraction of remaining capacity. Specific results for three
423 different emission times are reported in Table S3 in Supplementary Information-1

424

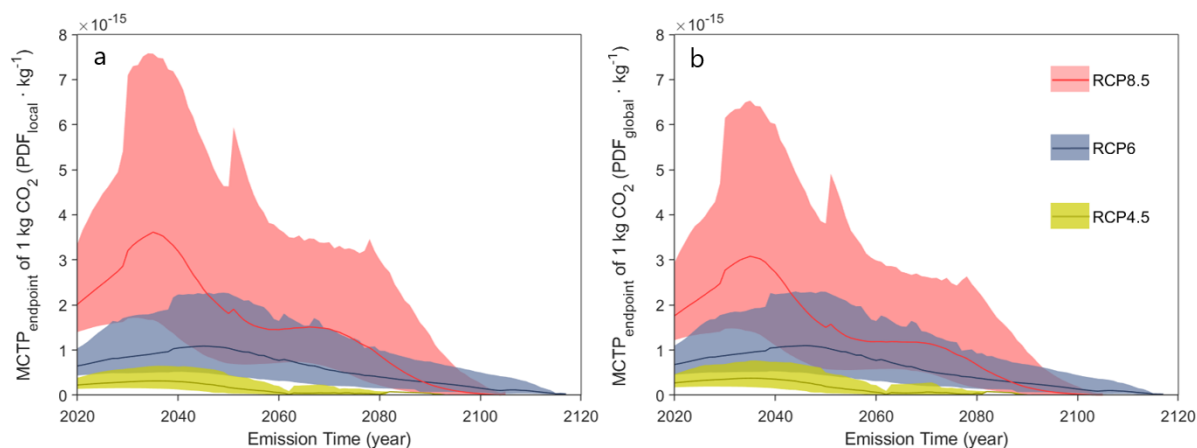
425 **3.2 Uncertainty and sensitivity**

426 When uncertainties about occurrence and timing of tipping points are accounted for with Monte Carlo
427 simulations, average (geometric mean) $MCTP_{\text{endpoint}}$ factors for both local and global species losses
428 are somewhat smoothed compared to a single iteration, indicating that uncertainties in the exact
429 location of the tipping point are so large that single tipping events are not clearly distinguishable (Fig.
430 4). Nevertheless, the fluctuations of the factors over time indicate that it is still possible to identify
431 periods with larger probability of crossing tipping points in proximity of the observed peaks. This
432 shows that, despite the uncertainties, impacts, and thus our CFs, still depend on the specific timing of
433 GHG emissions and thus on the proximity to tipping points. These findings are consistent with
434 observations noted in Fabbri et al. (2021) for the midpoint $MCTP$. Emissions between 2040 and 2060
435 have the largest potential to cause species loss as a consequence of crossing tipping points assuming
436 RCP6. The sharp peak around years 2050-2055 indicates that uncertainty around the tipping is lower
437 here, making the potential tipping time more identifiable. After this period, potential damage per unit
438 emission decreases, confirming the trend observed in the sample iteration. Average $MCTP_{\text{endpoint}}$
439 factors calculated for local and global species losses are numerically similar. Under RCP6, average
440 (geometric mean) $MCTP_{\text{endpoint}}$ factors based on local species loss range between $2.7 \cdot 10^{-17}$ and $1.1 \cdot 10^{-15}$
441 ¹⁵ PDF per 1 kg of CO₂, depending on the year of emission, with 90% of the iterations oscillating
442 between $2.2 \cdot 10^{-17}$ and $2.3 \cdot 10^{-15}$ PDF per unit emission (Fig. 4a). The $MCTP_{\text{endpoint}}$ factors for global
443 species losses can be up to 5% larger and 13% lower than results for local species loss, depending on
444 the emission year.

445 The comparison between RCP pathways shows that potential local and global species
446 losses per kg of CO₂ emitted are generally larger under RCP8.5 and lower under RCP4.5. $MCTP_{\text{endpoint}}$
447 factors for local species losses can be up to 4 and 87 times larger (depending on emission time) under

448 RCP8.5 compared to RCP6 and RCP4.5, respectively, whereas for global species losses they are up to
449 3 and 35 times larger than the other two pathways. This is consistent with expectations that more
450 species will be lost at higher temperature levels. Larger impacts under RCP8.5, in terms of
451 contribution of a GHG emission to crossing tipping points, were also found in Jørgensen et al. (2014),
452 who studied the influence of RCP pathway on their developed midpoint climate tipping metric. This
453 was due to the higher GHG concentration levels projected in this pathway, which reduced the
454 remaining atmospheric capacity up to the considered tipping point (Arctic summer sea ice).
455 Conversely, the result is in contrast with what reported in Fabbri et al. (2021), where midpoint
456 MCTPs for RCP8.5 were lower than those for RCP4.5. This reflects the inability of the midpoint
457 MCTPs to represent the potential larger impacts when temperature projections are higher and
458 highlights the relevance of performing damage modelling as presented here.

459 The different trends observed in the three RCPs are mainly explained by the different
460 number and timing of occurring tipping points, which in turn are determined by the level and
461 evolution of the global temperature projected in each RCP (see Table S1 in Supplementary
462 Information-1 for occurrence of tipping points depending on the RCPs). Under RCP8.5 impacts are
463 larger for emissions occurring within 2045, because a larger number of tipping points is expected to
464 be crossed within this period due to the rapid increase in temperatures projected in this pathway. The
465 number of potential tipping points in RCP6 and RCP4.5 is progressively lower, and their occurrence
466 is slightly postponed due to the lower rate of temperature increase (particularly for RCP6). Similar
467 trends are observed for CH₄ and N₂O, and MCTP_{endpoint} values for these two gases are on average 83
468 and 273 times larger, respectively, compared to those of CO₂ (Fig. S1)
469



470

471 **Fig. 4** Average (geometric mean) endpoint MCTP ($MCTP_{\text{endpoint}}$) of 1 kg of CO_2 based on local **(a)** and global
 472 **(b)** species loss (solid lines) and corresponding uncertainty ranges (shaded areas enclosed between the 5th and
 473 95th percentiles) calculated under RCP4.5, RCP6 and RCP8.5.

474

475 3.3 Findings from a case study

476 Ranking between plastic end-of-life scenarios obtained with the $MCTP_{\text{endpoint}}$ calculated in this study
 477 shows some differences when compared to ranking using the damage GWP-based metric (Table 2).

478 For the damage GWP, the lowest impacts are calculated when the plastic material degrades slowly
 479 enough so that the amount of GHGs emitted in 100 years is at a minimum, explaining why the very
 480 slowly and the fast-degrading plastics are the best and the worst scenarios respectively. This is also
 481 the case for our $MCTP_{\text{endpoint}}$ (for both local and global species losses) for very slowly degrading
 482 plastic, which is seen to have lowest impacts due to the very low amounts of GHGs emitted.

483 However, contrary to the GWP, where impacts are rather insensitive to biodegradation kinetics,
 484 climate tipping impacts also depend on emission timing, and are largest when emissions occur at the
 485 point in time where their contribution to cross tipping points is the largest (2040-2060). This

486 corresponds to fast biodegradation rate with a lag phase, followed by the scenario with medium
 487 biodegradation rate without a lag. These findings however do not necessarily show that slower
 488 degrading materials are always a better option (indeed the opposite is observed when comparing
 489 scenarios 2 and 4 under RCP6), but rather show that the performance depends on proximity of
 490 emissions to expected occurrence of tipping points. Ranking of scenarios from fast to slow

491 degradation rate differs slightly among the three RCP pathways, but the overall trends are the same,
 492 i.e. scenarios 3 (medium rate degradation) and 6 (20-years delayed degradation) are seen as the worst.
 493 The main difference here between RCP pathways is that $MCTP_{\text{endpoint}}$ scores calculated under RCP8.5
 494 are always higher than scores under the other two RCP pathways, reflecting potentially larger species
 495 loss in a high emissions pathway and, thus, the dependency of the product's performance on the
 496 chosen emission path.

497

498 **Table 2** Total impact scores per functional unit (f.u.) for the considered end-of-life scenarios according to
 499 endpoint MCTP ($MCTP_{\text{endpoint}}$) for both local and global species losses and the complementary metric of damage
 500 to ecosystems from ReCiPe 2016. The sequence green – yellow – red shading indicates ranking between
 501 scenarios (within columns), from lowest (green) to highest (red) impact scores

Scenario	$MCTP_{\text{endpoint}}$ for local species losses ($PDF_{\text{local}}/\text{f.u.}$)			$MCTP_{\text{endpoint}}$ for global species losses ($PDF_{\text{global}}/\text{f.u.}$)			Damage GWP (ReCiPe 2016) (Species · yr/f.u.)
	RCP4.5	RCP6	RCP8.5	RCP4.5	RCP6	RCP8.5	
1. Incineration	4.1E-16	1.2E-15	3.7E-15	5.0E-16	1.2E-15	3.2E-15	5.1E-09
Plastic degradation rate							
2. Fast	3.3E-15	7.8E-15	3.0E-14	4.0E-15	8.2E-15	2.6E-14	2.3E-08
3. Medium	4.2E-15	1.2E-14	4.3E-14	5.0E-15	1.2E-14	3.7E-14	2.3E-08
4. Slow	2.7E-15	1.0E-14	3.0E-14	3.2E-15	1.0E-14	2.5E-14	2.1E-08
5. Very slow	2.0E-17	9.0E-17	2.3E-16	2.3E-17	8.9E-17	1.9E-16	2.2E-10
Delayed degradation							
6. After 20 years (fast rate)	5.6E-15	1.7E-14	5.7E-14	6.5E-15	1.7E-14	4.8E-14	2.3E-08
7. After 50 years (fast rate)	1.2E-15	9.1E-15	2.7E-14	1.5E-15	8.7E-15	2.1E-14	2.3E-08

502

503

504 4 Discussion

505 4.1 Metrics based on ecosystem damage

506 The $MCTP_{\text{endpoint}}$ factors calculated here measure the potential loss of species biodiversity from a
 507 GHG emission that contributes to passing climate tipping points. We emphasize that this potential
 508 species loss should be seen as the translation of the contribution of an emission to tipping (expressed

509 at midpoint level) into the resulting potential loss of species. The focus here is on impacts through
510 contributions to climate tipping and not on assessing the biodiversity loss from GHG emissions
511 through the time-integrated radiative forcing impact pathway (linking radiative forcing change to
512 time-integrated temperature change and to final species loss) that is represented by the GWP-based
513 metric for ecosystem damage. Similarly, it is not the aim of the present method to assess tipping
514 points for critical loss of species.

515 In our model we have accounted for the acceleration of species loss with increasing
516 temperature levels in line with recent estimates (Newbold, 2018; Urban, 2015). Thus, we could have
517 expected the impact on species to be larger for future emissions (i.e. occurring at higher levels of
518 warming) than for emissions today, returning increasing $MCTP_{\text{endpoint}}$ results over time. However, we
519 found that this acceleration is counteracted by the simultaneous decline in the contribution of an
520 emission to temperature rise over time. As a unit emission of CO_2 leads to a lower temperature
521 increase when emitted closer to the year of the last tipping point, in line with the *average* approach to
522 modelling characterization factors, it follows that the impact on species diversity can be
523 proportionally lower for emissions occurring later, toward the end of the century. Therefore, the
524 resulting decrease in $MCTP_{\text{endpoint}}$ factors should not be interpreted as, e.g., lower sensitivity of the
525 climate to future emissions or other climate related mechanisms.

526 In contrast to other endpoint metrics (including damage GWP) that assess effects of
527 GHG emissions on biodiversity in LCA, the $MCTP_{\text{endpoint}}$ introduces a temporal perspective also in the
528 midpoint to endpoint factor. As a consequence, the $MCTP_{\text{endpoint}}$ for a specific gas depends on the
529 emission year. The results from the case study suggest that use of the new metric gives additional
530 insights about the performance of the compared products, capturing larger potential impacts when
531 emissions from the product occur in periods when probability of tipping points is the largest (between
532 2040 and 2060 under RCP6), distinguishing it from the damage GWP. This finding is in line with
533 what was found when applying the CFs at the midpoint level (Fabbri et al., 2021).

534 We find little difference between the $MCTP_{\text{endpoint}}$ factors that express local and global
535 species losses. This is due to the similarity of the curves used to describe local and global species loss
536 as function of temperature rise (Fig. 2). This observation seems at odds with the expectation that local

537 losses should be larger than global because a substantial local loss of species is likely to occur before
538 those species start becoming globally extinct. However, the outcome depends on the spatial
539 distribution of species and on which species are lost first. For instance, if the loss involves very
540 narrowly distributed species, then global extinctions could become high without having a large impact
541 on local diversity. Furthermore, the inclusion of some data on fish species (from 10 out of 131
542 assessed studies) slightly alters the representativeness of the study of Urban (2015) for modeling
543 terrestrial species losses and may have an influence on the similarity between local and global level
544 results. Finally, an additional reason could be that the estimates of global losses from the study of
545 Urban (2015), which were extrapolated from local and regional studies, are, in reality, more
546 representative for local species losses, explaining the similarity with figures from Newbold (2018).

547

548 **4.2 Applicability in life cycle assessment**

549 The emission year-specific $MCTP_{\text{endpoint}}$ factors for the three gases (CO_2 , CH_4 and N_2O) provided here
550 (Supplementary Information-2, Tables S1-S6) are directly applicable in LCA studies to assess the
551 potential species loss stemming from the life cycle of products or services. The added value of the
552 $MCTP_{\text{endpoint}}$ compared to other damage metrics used in LCA is to consider that larger potential
553 impacts on species could occur when emissions are released in periods with higher probability of
554 crossing tipping points. As opposite, tipping points and the dependency of impacts on emission timing
555 are ignored in other PDF-based calculations. This revealed new insights about the performance of
556 different plastics when compared to the damage GWP metric, highlighting the relevance of
557 considering climate tipping as a separate impact category. This has also the advantage of showing
558 when emissions associated to product life cycles should be mostly avoided, through e.g. carbon
559 storage in products, which could potentially delay the tipping and allow implementation of climate
560 change mitigation and/or adaptation solutions. As for the midpoint MCTP, use of $MCTP_{\text{endpoint}}$ is
561 relevant when a time-differentiated inventory is available for the assessed products. However, since
562 temporarily disaggregated inventories are not yet easy to implement into dominant LCA software,
563 calculation of $MCTP_{\text{endpoint}}$ impact scores (through eq. 6) has to be conducted offline. For situations

564 where temporal disaggregation of the inventories is not deemed relevant, we recommend using
565 $MCTP_{\text{endpoint}}$ factors calculated for single year (e.g. 2021) to match with aggregated emissions for the
566 same year.

567 Advancing the midpoint MCTP to endpoint level should ideally allow for comparison
568 with the damage caused by other environmental impacts, such as eutrophication or ecotoxicity but
569 also other climate-related impact categories (such as those based on the GWP). For instance,
570 comparison of our $MCTP_{\text{endpoint}}$ for global species losses with the damage GWPs from ReCiPe 2016
571 could be possible as the species loss considered in both MCTP and GWP-based methods are based on
572 global extinction risks of Urban (2015). However, for direct comparisons harmonization of units is
573 required. This requires two steps. In the first step, conversion of the potentially disappeared fraction
574 of species (used in $MCTP_{\text{endpoint}}$) to absolute number of species (used in methods such as ReCiPe
575 2016) is needed. For $MCTP_{\text{endpoint}}$ factors expressing global species losses, this can be done by
576 multiplying the final $MCTP_{\text{endpoint}}$ impact score of the assessed product (calculated through eq. 6) with
577 the total number of terrestrial species on the planet. This value is estimated to be approximately 6.5
578 million (Mora et al., 2011), of which 1.6 million are the species that have been classified (Goedkoop
579 et al., 2009). Even though the former value would be recommended as it gives a more realistic
580 measure of species diversity, the latter should be used when the purpose is to compare with ReCiPe
581 2016 (as this is the value adopted in ReCiPe). Conversion to absolute losses for the $MCTP_{\text{endpoint}}$
582 factors expressing local species losses is considered less relevant for comparisons with other impact
583 categories, due to lack of existing damage metrics expressed as absolute local species losses, and thus
584 it was not carried out here. We stress however that in this case a different calculation approach would
585 be needed. It would require recalculation of the $MCTP_{\text{endpoint}}$ factors using estimates of absolute
586 (rather than fractional) local species losses per temperature change, obtained as an average over each
587 grid cell considered in Newbold (2018).

588 The second step addresses the time (exposure duration), which is not explicit in the
589 $MCTP_{\text{endpoint}}$ unit. Other damage-oriented CFs include a time dimension when expressing impacts on
590 biodiversity, e.g., species·yr (ReCiPe 2016) or PDF·yr (LC-IMPACT), which may represent the
591 duration (in years) of the period of exposure to the pressure (e.g. the residence time of the emission in

592 the environment). To harmonize the units of the $MCTP_{\text{endpoint}}$ with other damage-oriented metrics, an
593 idea could be to multiply the $MCTP_{\text{endpoint}}$ impact scores (in either PDF or species) by the total number
594 of years from the first emission up to the last expected tipping point in each RCP pathway. This
595 number corresponds to 70, 97 and 85 years for RCP4.5, RCP6 and RCP8.5, respectively, for
596 emissions starting in year 2021. We recall that in RCP4.5 the global temperature starts to stabilize at
597 around 2.5° C within 70 years, meaning that tipping points expected at higher temperature levels
598 cannot occur after this time, whereas for the other two pathways the temperature projections keep
599 increasing and later tipping points could be expected. The resulting $MCTP_{\text{endpoint}}$ impact scores for the
600 case study therefore become 2-3 orders magnitude higher when compared to scores obtained using
601 damage GWPs.

602

603 **4.3 Limitations**

604 One limitation in the midpoint to endpoint factor is that the uncertainties related to estimation of
605 species loss with temperature change were not considered. Accounting for modelling uncertainties
606 Newbold (2018) reports that temperature increases between 2.5 and 4.8°C (relative to pre-industrial)
607 would lead to changes in local species numbers ranging between a 2% gain and 47% loss (overall
608 figures across all used RCP scenarios and species distribution modelling algorithms). For global
609 species losses, uncertainties across the individual studies considered by Urban (2015) for similar
610 temperature increases (2 - 4.3°C relative to pre-industrial) range from about 4 to 20%.

611 Second, given the dependency of the damage $MCTP$ factors on the number of
612 considered climate tipping points, a limitation is our lack of knowledge about all potential present and
613 future tipping points. Our framework uses the current knowledge about tipping points, but it can be
614 readily updated when additional potential tipping points are discovered.

615 A third limitation is the inability of the damage $MCTP$ factors to capture the full
616 impacts from climate tipping. The models used to estimate species loss only capture direct effects of
617 temperature increases, and do not consider other impacts of crossing the tipping points, such as major
618 biome shifts, monsoon shifts or Amazon forest dieback. The way in which species could respond to,

619 e.g. a recurring ice-free summer in the Arctic, or a gradual but irreversible dieback of the Amazon
620 forest is difficult to predict (Post et al., 2009). Several models assessing the impacts of future climate
621 change on biodiversity have been developed (see e.g. Pearson and Dawson, 2003; Thuiller et al.,
622 2013), but estimates of the consequences of specific tipping events are lacking or incomplete. For this,
623 direct impacts such as those derived from loss or degradation of the natural habitat of species, e.g.,
624 biodiversity loss from forest dieback or intensified droughts, and the influence that these may have on
625 the fraction of species loss per unit of temperature increase were not considered. This implies that the
626 impacts calculated through the damage MCTP factors are probably underestimated.

627 Fourth, there is a limitation in the way in which the temperature rise following a
628 tipping event was determined. This measure depends on several uncertain factors, such as the
629 potential consequences on the climate from tipping, the rate at which the consequences unfold and the
630 response of the climate to these changes. We used available estimates of carbon emissions and
631 relative radiative forcing change caused by tipping, but no uncertainty estimates were included as they
632 are rarely available. In addition, the approach adopted to calculate the temperature increase following
633 carbon emissions, which in practice assumes that temperature increases faster but never exceeding the
634 projection of each RCP pathway, is an oversimplification of the climate mechanisms involved. A
635 more appropriate measure would require the use of climate models simulating the climate-carbon-
636 cycle system, such as Earth system models (ESMs) (Millar et al., 2017). The main implication of
637 these model limitations is to underestimate the potential temperature increase induced by passing
638 tipping points, which could actually rise above RCP projections, and, consequently, indicate an
639 underestimation of the resulting loss of species. This may affect the magnitude of $MCTP_{\text{endpoint}}$ factors
640 to some extent, but it is not expected to change the observed overall trends.

641

642 **4.3.1 Priorities for further developments**

643 As every biodiversity loss metric focusing only on the loss of species diversity, our metric assigns an
644 equal weight to all species without considering e.g. the functional role that species play in the
645 ecosystem, assuming that the damage to biodiversity is independent of which species are lost.

646 However, in terms of consequences for the natural ecosystems, it is not given that all species should
647 be weighted equally, and furthermore it is not given that species which remain in the future should
648 have the same weight as species living today. For example, losing species in the future, when many
649 others have already disappeared, may compromise the ecosystems' functions more severely than
650 when species diversity is still (relatively) high, as of today. Further, the loss of keystone species,
651 playing a critical role in the ecosystem, may weight more than a larger decline of species performing
652 less crucial functions. Complex interactions exist between species in ecological communities and, for
653 this, the loss of certain critical species from a community could cause a cascade of secondary
654 extinctions of many other species (Brodie et al., 2014; Dunne and Williams, 2009). Ideally these
655 dynamics could be included in our metric by introducing a *severity* factor in eq. 1, providing a
656 measure of severity of the damage. As the current ability to predict these mechanisms in the ecology
657 and climate fields is rather limited, however, calculation of such a severity factor is not
658 straightforward.

659

660 **5 Conclusions**

661 Our work is the first attempt to link midpoint multiple climate tipping points metrics of GHG
662 emissions to loss of terrestrial species biodiversity at local and global scales. The developed
663 $MCTP_{\text{endpoint}}$ metric attributes a larger potential species loss to emissions occurring when their
664 contribution to crossing tipping points is higher, given that crossing could intensify warming and
665 further exacerbate species loss. Therefore, the main advantage of the $MCTP_{\text{endpoint}}$ compared to the
666 midpoint $MCTP$ is to express impacts in terms of damage to terrestrial species. Overall, $MCTP_{\text{endpoint}}$
667 values decrease over time, meaning that emissions occurring later in the century are attributed a lower
668 potential species loss. This decline is found to depend on the decreasing contribution of emissions to
669 temperature rise over time, even though acceleration of species loss with increasing temperature
670 levels has been accounted for.

671 The $MCTP_{\text{endpoint}}$ can be used in LCA to assess the potential loss of terrestrial species
672 stemming from the life cycle of products. Application of the metric is considered particularly valuable

673 for products where time-differentiation of emissions is relevant, such as biodegradable plastics or
674 deteriorating wooden products. The $MCTP_{\text{endpoint}}$ complements existing damage-level metrics used in
675 LCIA and we therefore recommend including it as new damage category. For consistency with other
676 damage metrics expressing global species loss impacts, we recommend using $MCTP_{\text{endpoint}}$ values
677 predicting global species loss. It is also recommended to present results for all three considered RCP
678 scenarios as a sensitivity analysis. Differences in how time is treated in $MCTP_{\text{endpoint}}$, however, when
679 compared to other damage metrics used in LCA warrant further harmonization efforts. In the broader
680 LCA context, our $MCTP_{\text{endpoint}}$ penalizes emissions occurring closer to tipping points, particularly
681 those occurring between 2040 and 2060. Their use thus aims to discourage emissions attributed to
682 product life cycles that will occur when they matter most and result in largest damage, offering the
683 possibility to postpone the tipping, e.g. through carbon storage in products, thus buying time for the
684 implementation of climate change mitigation and/or adaptation solutions (Jørgensen et al., 2015).

685

686 **Supplementary Information**

687 Supplementary methods and results (Supplementary Information-1)

688 Emission-year specific $MCTP_{\text{endpoint}}$ values (Supplementary Information-2)

689

690 **Data availability statement**

691 All data generated during this study are included in this published article [and its supplementary
692 information files].

693

694 **Funding**

695 This work was financially supported by the European Commission under Horizon 2020; H2020-BBI-
696 JTI-2016: BioBarr, grant agreement 745586.

697

698 **Declarations**

699 **Conflict of interest.** The authors have no competing interests to declare.

700

701 **References**

702 Bjørn, A., Owsianiak, M., Molin, C., Laurent, A., 2018. Main Characteristics of LCA., in: Hauschild,
703 M.Z., Rosenbaum, R.K., Olsen, S.I. (Eds.), Life Cycle Assessment: Theory and Practice. Cham,
704 Eds.; Springer International Publishing:, pp. 9–16. [https://doi.org/https://doi.org/10.1007/978-3-](https://doi.org/https://doi.org/10.1007/978-3-319-56475-3_2)
705 [319-56475-3_2](https://doi.org/https://doi.org/10.1007/978-3-319-56475-3_2)

706 Brodie, J.F., Aslan, C.E., Rogers, H.S., Redford, K.H., Maron, J.L., Bronstein, J.L., Groves, C.R.,
707 2014. Secondary extinctions of biodiversity. *Trends Ecol. Evol.* 29, 664–672.
708 <https://doi.org/10.1016/j.tree.2014.09.012>

709 Cho, H.S., Moon, H.S., Kim, M., Nam, K., Kim, J.Y., 2011. Biodegradability and biodegradation rate
710 of poly (caprolactone) -starch blend and poly (butylene succinate) biodegradable polymer
711 under aerobic and anaerobic environment. *Waste Manag.* 31, 475–480.
712 <https://doi.org/10.1016/j.wasman.2010.10.029>

713 Collen, B., Böhm, M., Kemp, R., Baillie, J.E.M., 2012. Spineless: status and trends of the world's
714 invertebrates. Zoological Society of London, United Kingdom.

715 Curran, M., De Baan, L., De Schryver, A.M., Van Zelm, R., Hellweg, S., Koellner, T., Sonnemann,
716 G., Huijbregts, M.A.J., 2011. Toward meaningful end points of biodiversity in life cycle
717 assessment. *Environ. Sci. Technol.* 45, 70–79. <https://doi.org/10.1021/es101444k>

718 Dunne, J.A., Williams, R.J., 2009. Cascading extinctions and community collapse in model food
719 webs. *Philos. Trans. R. Soc. B Biol. Sci.* 364, 1711–1723.
720 <https://doi.org/10.1098/rstb.2008.0219>

721 Elith, J., Leathwick, J.R., 2009. Species Distribution Models: Ecological Explanation and Prediction

722 Across Space and Time. *Annu. Rev. Ecol. Evol. Syst.* 40, 677–697.
723 <https://doi.org/10.1146/annurev.ecolsys.110308.120159>

724 Fabbri, S., Hauschild, M.Z., Lenton, T.M., Owsianiak, M., 2021. Multiple climate tipping points
725 metrics for improved sustainability assessment of products and services. *Environ. Sci. Technol.*
726 55, 2800–2810. <https://doi.org/10.1021/acs.est.0c02928>

727 Goedkoop, M., Heijungs, R., Huijbregts, M., Schryver, A. De, Struijs, J., Zelm, R. Van, 2009. ReCiPe
728 2008 -A life cycle impact assessment method which comprises harmonised category indicators
729 at the midpoint and the endpoint level. Report 1: Characterization.

730 Hauschild, M.Z., Huijbregts, M.A.J., 2015. Life Cycle Impact Assessment, in: Klopffer, W., Curran,
731 M.A. (Eds.), *LCA Compendium – The Complete World of Life Cycle Assessment*, Springer.

732 Huijbregts, M.A.J., Steinmann, Z.J.N., Elshout, P.M.F., Stam, G., Verones, F., Vieira, M., Zijp, M.,
733 Hollander, A., van Zelm, R., 2017. ReCiPe2016 : a harmonised life cycle impact assessment
734 method at midpoint and endpoint level. *Int. J. Life Cycle Assess.* 22, 138–147.
735 <https://doi.org/10.1007/s11367-016-1246-y>

736 Ishigaki, T., Sugano, W., Nakanishi, A., Tateda, M., Ike, M., Fujita, M., 2004. The degradability of
737 biodegradable plastics in aerobic and anaerobic waste landfill model reactors. *Chemosphere* 54,
738 225–233. [https://doi.org/10.1016/S0045-6535\(03\)00750-1](https://doi.org/10.1016/S0045-6535(03)00750-1)

739 Jolliet, O., Antón, A., Boulay, A., Cherubini, F., Fantke, P., Levasseur, A., Mckone, T.E., Michelsen,
740 O., Milà, L., Motoshita, M., 2018. Global guidance on environmental life cycle impact
741 assessment indicators : impacts of climate change , fine particulate matter formation , water
742 consumption and land use. *Int. J. Life Cycle Assess.* 23, 2189–2207.

743 Jørgensen, S. V., Hauschild, M.Z., Nielsen, P.H., 2015. The potential contribution to climate change
744 mitigation from temporary carbon storage in biomaterials. *Int. J. Life Cycle Assess.* 20, 451–
745 462. <https://doi.org/10.1007/s11367-015-0845-3>

746 Jørgensen, S. V., Hauschild, M.Z., Nielsen, P.H., 2014. Assessment of urgent impacts of greenhouse

747 gas emissions - The climate tipping potential (CTP). *Int. J. Life Cycle Assess.* 19, 919–930.
748 <https://doi.org/10.1007/s11367-013-0693-y>

749 Lenton, T.M., Held, H., Kriegler, E., Hall, J.W., Lucht, W., Rahmstorf, S., Schellnhuber, H.J., 2008.
750 Tipping elements in the Earth's climate system. *Proc. Natl. Acad. Sci.* 105, 1786–1793.
751 <https://doi.org/10.1073/pnas.0705414105>

752 Meinshausen, M., Smith, S.J., Calvin, K., Daniel, J.S., Kainuma, M.L.T., Lamarque, J., Matsumoto,
753 K., Montzka, S.A., Raper, S.C.B., Riahi, K., Thomson, A., Velders, G.J.M., van Vuuren, D.P.P.,
754 2011. The RCP greenhouse gas concentrations and their extensions from 1765 to 2300. *Clim.*
755 *Change* 109, 213–241. <https://doi.org/10.1007/s10584-011-0156-z>

756 Millar, J.R., Nicholls, Z.R., Friedlingstein, P., Allen, M.R., 2017. A modified impulse-response
757 representation of the global near-surface air temperature and atmospheric concentration response
758 to carbon dioxide emissions. *Atmos. Chem. Phys.* 17, 7213–7228. [https://doi.org/10.5194/acp-](https://doi.org/10.5194/acp-17-7213-2017)
759 [17-7213-2017](https://doi.org/10.5194/acp-17-7213-2017)

760 Mora, C., Tittensor, D.P., Adl, S., Simpson, A.G.B., Worm, B., 2011. How many species are there on
761 earth and in the ocean? *PLoS Biol.* 9, 1–8. <https://doi.org/10.1371/journal.pbio.1001127>

762 Newbold, T., 2018. Future effects of climate and land-use change on terrestrial vertebrate community
763 diversity under different scenarios. *Proc. R. Soc. B Biol. Sci.* 285.
764 <https://doi.org/10.1098/rspb.2018.0792>

765 Pearson, R.G., Dawson, T.P., 2003. Predicting the impacts of climate change on the distribution of
766 species: Are bioclimate envelope models useful? *Glob. Ecol. Biogeogr.* 12, 361–371.
767 <https://doi.org/10.1046/j.1466-822X.2003.00042.x>

768 Post, E., Forchhammer, M.C., Bret-Harte, M.S., Callaghan, T. V., Christensen, T.R., Elberling, B.,
769 Fox, A.D., Gilg, O., Hik, D.S., Høye, T.T., Ims, R.A., Jeppesen, E., Klein, D.R., Madsen, J.,
770 McGuire, A.D., Rysgaard, S., Schindler, D.E., Stirling, I., Tamstorf, M.P., Tyler, N.J.C., Van
771 Der Wal, R., Welker, J., Wookey, P.A., Schmidt, N.M., Aastrup, P., 2009. Ecological dynamics

772 across the arctic associated with recent climate change. *Science* (80-). 325, 1355–1358.
773 <https://doi.org/10.1126/science.1173113>

774 Purvis, A., 2020. A single apex target for biodiversity would be bad news for both nature and people.
775 *Nat. Ecol. Evol.* 4, 768–769. <https://doi.org/10.1038/s41559-020-1181-y>

776 Rossi, V., Cleeve-Edwards, N., Lundquist, L., Schenker, U., Dubois, C., Humbert, S., Jolliet, O.,
777 2015. Life cycle assessment of end-of-life options for two biodegradable packaging materials:
778 Sound application of the European waste hierarchy. *J. Clean. Prod.* 86, 132–145.
779 <https://doi.org/10.1016/j.jclepro.2014.08.049>

780 Sanford, T., Frumhoff, P.C., Luers, A., Gullede, J., 2014. The climate policy narrative for a
781 dangerously warming world. *Nat. Clim. Chang.* 4, 164–166.
782 <https://doi.org/10.1038/nclimate2148>

783 Steffen, W., Rockström, J., Richardson, K., Lenton, T.M., Folke, C., Liverman, D., Summerhayes,
784 C.P., Barnosky, A.D., Cornell, S.E., Crucifix, M., Donges, J.F., Fetzer, I., Lade, S.J., Scheffer,
785 M., Winkelmann, R., Schellnhuber, H.J., 2018. Trajectories of the Earth System in the
786 Anthropocene. *Proc. Natl. Acad. Sci.* 115, 8252–8259. <https://doi.org/10.1073/pnas.1810141115>

787 Tansel, B., 2019. Persistence times of refractory materials in landfills: A review of rate limiting
788 conditions by mass transfer and reaction kinetics. *J. Environ. Manage.* 247, 88–103.
789 <https://doi.org/10.1016/j.jenvman.2019.06.056>

790 Thuiller, W., Münkemüller, T., Lavergne, S., Mouillot, D., Mouquet, N., Schiffers, K., Gravel, D.,
791 2013. A road map for integrating eco-evolutionary processes into biodiversity models. *Ecol.*
792 *Lett.* 16, 94–105. <https://doi.org/10.1111/ele.12104>

793 Urban, M.C., 2015. Accelerating extinction risk from climate change. *Science* (80-). 348, 571–573.
794 <https://doi.org/10.1126/science.aaa4984>

795 van Vliet, J., den Elzen, M.G.J., van Vuuren, D.P., 2009. Meeting radiative forcing targets under
796 delayed participation. *Energy Econ.* 31, S152–S162. <https://doi.org/10.1016/j.eneco.2009.06.010>

797 van Vuuren, D.P., Edmonds, J., Kainuma, M., Riahi, K., Thomson, A., Hibbard, K., Hurtt, G.C.,
798 Kram, T., Krey, V., Lamarque, J.-F., Masui, T., Meinshausen, M., Nakicenovic, N., Smith, S.J.,
799 Rose, S.K., 2011. The representative concentration pathways: an overview. *Clim. Change* 109,
800 5–31. <https://doi.org/10.1007/s10584-011-0148-z>

801 Verones, F., Hellweg, S., Antón, A., Azevedo, L.B., Chaudhary, A., Cosme, N., Cucurachi, S., de
802 Baan, L., Dong, Y., Fantke, P., Golsteijn, L., Hauschild, M., Heijungs, R., Jolliet, O., Juraske,
803 R., Larsen, H., Laurent, A., Mutel, C.L., Margni, M., Núñez, M., Owsianiak, M., Pfister, S.,
804 Ponsioen, T., Preiss, P., Rosenbaum, R.K., Roy, P.O., Sala, S., Steinmann, Z., van Zelm, R., Van
805 Dingenen, R., Vieira, M., Huijbregts, M.A.J., 2020. LC-IMPACT: A regionalized life cycle
806 damage assessment method. *J. Ind. Ecol.* 1–19. <https://doi.org/10.1111/jiec.13018>

807 Verones, F., Huijbregts, M.A.J., Azevedo, L.B., Chaudhary, A., Baan, L. De, Fantke, P., Hauschild,
808 M., Henderson, A.D., Mutel, C.L., Owsianiak, M., Pfister, S., Preiss, P., Roy, O., Scherer, L.,
809 Steinmann, Z., Zelm, R. Van, Dingenen, R. Van, 2019. LC-IMPACT Version 1.0 - A spatially
810 differentiated life cycle impact assessment approach [WWW Document]. URL [https://lc-](https://lc-impact.eu/)
811 [impact.eu/](https://lc-impact.eu/) (accessed 8.9.20).

812 Woods, J.S., Damiani, M., Fantke, P., Henderson, A.D., Johnston, J.M., Bare, J., Sala, S., Maia de
813 Souza, D., Pfister, S., Posthuma, L., Rosenbaum, R.K., Verones, F., 2018. Ecosystem quality in
814 LCIA: status quo, harmonization, and suggestions for the way forward. *Int. J. Life Cycle Assess.*
815 23, 1995–2006. <https://doi.org/10.1007/s11367-017-1422-8>

816